energy&fuels

Article

pubs.acs.org/EF

Investigation of Iso-octane Ignition and Validation of a Multizone Modeling Method in an Ignition Quality Tester

Eric M. Osecky,*[†] Gregory E. Bogin, Jr.,[†] Stephanie M. Villano,[†] Matthew A. Ratcliff,[‡] Jon Luecke,[‡] Bradley T. Zigler,[‡] and Anthony M. Dean[†]

[†]Colorado School of Mines, 1610 Illinois Street, Golden, Colorado 80401, United States

[‡]National Renewable Energy Laboratory, 15013 Denver West Parkway, Golden, Colorado 80401, United States

Ⓢ *Supporting Information*

ABSTRACT: An ignition quality tester was used to characterize the autoignition delay times of iso-octane. The experimental data were characterized between temperatures of 653 and 996 K, pressures of 1.0 and 1.5 MPa, and global equivalence ratios of 0.7 and 1.05. A clear negative temperature coefficient behavior was seen at both pressures in the experimental data. These data were used to characterize the effectiveness of three modeling methods: a single-zone homogeneous batch reactor, a multizone engine model, and a three-dimensional computational fluid dynamics (CFD) model. A detailed 874 species iso-octane ignition mechanism (Mehl, M.; Curran, H. J.; Pitz, W. J.; Westbrook, C. K. Chemical kinetic modeling of component mixtures relevant to gasoline. *Proceedings of the European Combustion Meeting*; Vienna, Austria, April 14−17, 2009) was reduced to 89 species for use in these models, and the predictions of the reduced mechanism were consistent with ignition delay times predicted by the detailed chemical mechanism across a broad range of temperatures, pressures, and equivalence ratios. The CFD model was also run without chemistry to characterize the extent of mixing of fuel and air in the chamber. The calculations predicted that the main part of the combustion chamber was fairly well-mixed at longer times (> ∼30 ms), suggesting that the simpler models might be applicable in this quasi-homogeneous region. The multizone predictions, where the combustion chamber was divided into 20 zones of temperature and equivalence ratio, were quite close to the coupled CFD−kinetics results, but the calculation time was ∼11 times faster than the coupled CFD−kinetics model. Although the coupled CFD−kinetics model captured the observed negative temperature coefficient behavior and pressure dependence, discrepancies remain between the predictions and the observed ignition time delays, suggesting improvements are still needed in the kinetic mechanism and/or the CFD model. This approach suggests a combined modeling approach, wherein the CFD calculations (without chemistry) can be used to examine the sensitivity of various model inputs to in-cylinder temperature and equivalence ratios. These values can be used as inputs to the multizone model to examine the impact on ignition delay. The speed of the multizone model also makes it feasible to quickly test more detailed kinetic mechanisms for comparison to experimental data and sensitivity analysis.

1. INTRODUCTION

The increasing demand for liquid transportation fuels, along with the goals of minimizing greenhouse gas emissions from fossil fuels and the dependence upon foreign energy sources, has led to an increase in interest in more energy-efficient engines and renewable liquid fuels. Advanced combustion engines, such as reactivity-controlled compression ignition (RCCI) engines, have shown promise for higher thermal efficiencies while lowering NO_x and soot emissions when compared to traditional diesel engines.[1] The ability to control the ignition timing in these advanced engines is dependent upon the autoignition kinetics of the fuel, which means that the development and validation of detailed chemical kinetic mechanisms will be very important in their design.[2] Many detailed chemical kinetic models for combustion of fuels have been developed,[3,4] but many of these mechanisms have not been well validated with experimental data, under engine-like conditions, especially mechanisms for low-volatility fuels.

Ignition characterization of low-volatility fuels by traditional methods (e.g., shock tubes, rapid compression machines, flow reactors, and jet-stirred reactors) can be difficult, although there have been advances in performing experiments with low-volatility fuels in rapid compression machines,[5] shock tubes,[6−8] and jet-stirred reactors.[9] In contrast, the ignition quality tester (IQT) can easily perform experiments on low-volatility fuel components and blends, and it has the potential, when suitably modified, to serve as a validation tool for kinetic models of low-volatility fuels. However, the ease of performing experiments on low-volatility fuels also comes with the added complication that fuel droplet breakup, evaporation, and mixing can also affect the ignition delay times of fuels.

The IQT is a constant volume combustion apparatus designed to measure the derived cetane number of fuels using the ASTM D6890 standard.[10] The combustion chamber can operate at pressures and temperatures that are similar to a diesel engine at top dead center. Because fuel is injected directly into the combustion chamber, experiments can easily be performed on low-volatility fuels. The IQT requires small amounts of fuel (<50 mL for derived cetane number measurement), making it ideal for measuring the ignition properties of emerging renewable fuels, which may only be available in small quantities. The IQT has been used previously

Received: June 8, 2016
Revised: August 16, 2016

DOI: 10.1021/acs.energyfuels.6b01406
Energy Fuels XXXX, XXX, XXX−XXX

by the authors and others to characterize the ignition delay times of various fuels across a broad range of conditions.[11−15] Also, the IQT has been used to compare ignition data with a homogeneous charge compression ignition engine.[16]

A coupled computational fluid dynamics (CFD)−kinetics analysis of the IQT has been carried out for *n*-heptane using the KIVA-3V software package.[17] This model used a 42 species skeletal *n*-heptane mechanism developed by Ra and Reitz.[18] Comparisons of the predicted and experimental ignition delay times are shown in Figure 1.

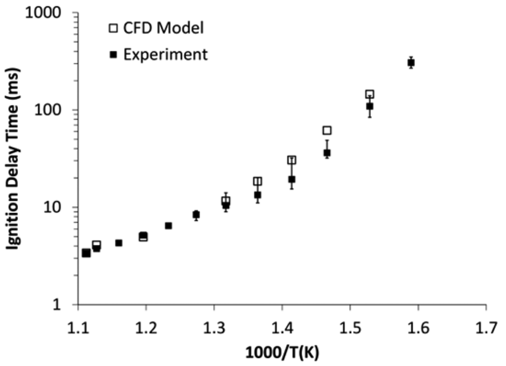

Figure 1. Comparison of IQT model-predicted ignition delay times and measured ignition delay times for *n*-heptane ($\Phi_{global} = 0.5$, $P = 2.1$ MPa, and 21% O_2): (□) KIVA model and (■) IQT experiment. This figure was reproduced with permission from ref 17. Copyright 2014 American Chemical Society.

This CFD model was able to predict the ignition delay times well at short times (<10 ms), suggesting that the spray breakup, evaporation, and mixing were accurately modeled using CFD. Similarly, the overall agreement at longer ignition delay times suggests that the mechanism used properly described the ignition kinetics. The overall agreement was encouraging, but extension of the coupled approach (CFD and ignition kinetics) to more complex fuels (which require larger mechanisms) and longer ignition delays is severely limited by the dramatic increase in computational time requirements.

One approach to substantially reducing the computational effort is to identify conditions where the ignition delay time is determined largely by the chemical kinetics with minimum impact from spray physics. Previous work by our group[19] characterized the ignition behavior of heptane isomers in the IQT. By modification of the experimental conditions, the ignition event could be delayed, allowing for the chemical kinetics, rather than spray physics, to dominate the ignition event. In fact, under conditions where the ignition delay time was long ($\gtrsim$20 ms), a negative temperature coefficient (NTC) behavior was observed in the IQT, indicating the influence of the chemical kinetics. A CFD analysis that characterized the fuel spray, droplet breakup, and fuel evaporation (no chemistry) was used to characterize the mixing inside the combustion chamber. These simulations predicted that a quasi-homogeneous region was formed in the main part of the IQT combustion chamber at long times ($\gtrsim$20 ms).[19] The temperature of this region was ∼60 K cooler than the initial temperature of the chamber, as a result of evaporative cooling of the fuel, and the local equivalence ratio was ∼1.5 times larger than the global equivalence ratio. These results suggested that a zero-dimensional (0D) homogeneous batch reactor model, using these adjusted initial conditions, might be used to model ignition inside the IQT at these long times. Such an approach would allow for a straightforward way to validate comprehensive kinetic mechanisms, because attempts to incorporate such detailed kinetics in a CFD analysis are typically very computationally intensive.

This approach of using a 0D homogeneous batch reactor was initially attempted for the heptane isomer experiments.[19] The mechanism used was developed by Westbrook and co-workers.[3] To bracket the expected equivalence ratio, 0D model predictions for heptane isomers were performed at both the global ratio and double that ratio. Experimental temperatures were adjusted to account for the evaporative cooling using a thermocouple that read 20−40 K cooler, instead of using the hottest thermocouple in the combustion chamber. Figure 2a shows that the predictions for one of the heptane isomers, 2,2,3-trimethylbutane, were able to capture the experimental data in terms of both the NTC behavior and the effect of the pressure. This was the least reactive isomer, and ignition delay times in the observed NTC region were greater than 60 ms for all three pressures. The model predictions for 2,3-dimethylpentane, a more reactive isomer, exhibited more deviations, as shown in Figure 2b. Some of the deviation can be readily explained by the expected impact of the physics at earlier ignition times. There have been several improvements made to the rate rules for branched alkane ignition in iso-octane chemical mechanisms[4,20] that were made after the development of the heptane isomer mechanism. While this suggests that some of the discrepancy would come from

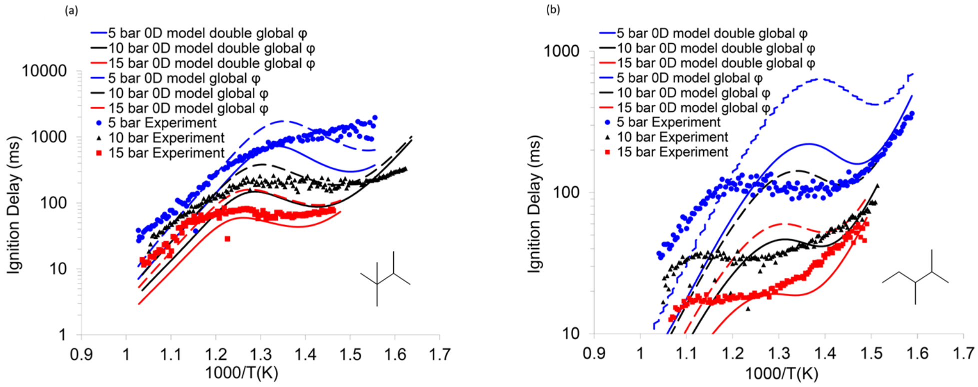

Figure 2. Experimental data (points) and model predictions (lines) for (a) 2,2,3-trimethylbutane and (b) 2,3-dimethylpentane at (blue) 0.5 MPa, (red) 1.0 MPa, and (black) 1.5 MPa. This figure was reproduced with permission from ref 19. Copyright 2013 American Chemical Society.

old rate rules, the systematic prediction of longer ignition delay times than experimentally observed at the lower temperatures suggests that issues remain with respect to inadequate description of the actual conditions inside the combustion chamber and that the single zone approach was not adequate.

To address these issues with model accuracy, this work considers iso-octane as the fuel. Although iso-octane is not a low-volatility fuel, its use provides several advantages: (1) This fuel is less reactive and has longer ignition delay times, allowing the IQT to be operated in a regime where chemical kinetics are expected to dominate. (2) Substantial research has been performed on both experiments and model development for iso-octane. Ignition data have been measured in multiple types of experiments, including shock tubes, rapid compression machines, and a jet-stirred reactor.[21−31] These data have been used to validate a detailed chemical kinetic mechanism for oxidation kinetics of iso-octane developed at Lawrence Livermore National Laboratory.[4,20,32] This mechanism has accurately predicted experimental data in these homogeneous experiments across pressures of 0.3−5.1 MPa, temperatures of 650−1200 K, and equivalence ratios of 0.3−1. This paper presents IQT experimental data gathered from 653 to 996 K, from 1.0 to 1.5 MPa, and a global equivalence ratio ranging from 0.7 to 1.05, generally within the ranges studied in homogeneous experiments. However, it should be noted that, while the variation in the global equivalence ratio extends slightly outside the range, there will likely be some regions inside the combustion chamber with an equivalence ratio higher than the global value. This presents the opportunity to extend the mechanism validation into fuel-rich conditions.

In this current paper, an improved description of the actual conditions inside the IQT is modeled by extending the single-zone 0D model, which was used earlier for the heptane isomers, to a multizone model. In both cases, the CFD model was run without chemistry (referred to here as CFD-without-chemistry) and was used to characterize temperatures and equivalence ratios at specified times, which are used as inputs for the single-zone and multizone simulations. These simulations are compared to a fully coupled CFD−kinetic analysis. The objective is to determine if a multizone model is adequate to predict the experimental results at longer ignition delay times. Also, the multizone model and coupled CFD−kinetics model will be compared to see if they give similar ignition delay time predictions. If so, this multizone model provides an approach whereby much larger detailed chemical mechanisms could be combined with the CFD-without-chemistry results to explore whether any remaining discrepancies could be addressed with a more complex kinetics model.

2. EXPERIMENTAL SECTION

The IQT, shown in Figure 3, is a constant-volume combustion apparatus with a spray injection system. Experimental parameters, such as the initial temperature, pressure, mass of fuel injected, and oxygen concentration, are well-controlled. The chamber is charged with air to a given pressure, where it is heated to the experimental temperature before fuel injection. Fuel is injected into the hot air, and ignition is measured by a pressure transducer (Kistler 601B1) at the rear of the combustion chamber. The fuel injector is a S-type inward-opening pintle-type injector with a single hole. The injection event is measured by a needle lift sensor that measures injector displacement. The ignition delay time is defined as the time between the start of fuel injection and the time when the pressure exceeds a set threshold above the initial pressure. For this study, the pressure threshold was set to 413 kPa above the initial pressure (the pressure threshold of the ASTM D6890 method is ∼138 kPa above the initial pressure). This higher pressure threshold was used so that ignition was not falsely detected during the chamber pressure rise caused by low-temperature heat release. Several modifications, including an independent control system, have been made to the IQT to more accurately study chemical kinetics. The independent control system used a National Instruments CompactDAQ data acquisition and control system to control chamber valves, start of fuel injection, and resetting of the pressure amplifier. Omega K-type thermocouples, with an accuracy of 0.75%, were used measure temperatures inside the combustion chamber. The IQT apparatus used for this study along with these modifications has been described previously in more detail.[11,19,33]

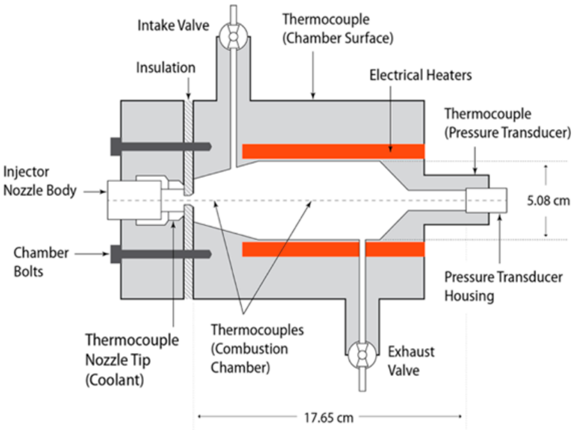

Figure 3. Schematic of the IQT combustion chamber.

The mass of fuel injected was varied between the two pressures by changing the thickness of shim in the injection pump. Masses of 55 and 83 mg of fuel were injected at 1.0 and 1.5 MPa, respectively. The temperature is measured by a thermocouple in the middle of the chamber and is a representative temperature of the majority of the chamber. The fuel injector and pressure transducer are cooled, resulting in sharp temperature gradients (ΔT = 400−700 K) near these devices.

Iso-octane was supplied by Sigma-Aldrich with a purity of 99.8%. High-purity gas was used to charge the combustion chamber. Synthetic air (20.9% oxygen with the balance being nitrogen) was used.

3. MODELING METHODS

3.1. CFD Model. A CFD model using the CONVERGE software package[34] was used to characterize fuel−air mixing and ignition inside the IQT. The CFD model couples fuel spray breakup and evaporation, turbulent mixing, heat transfer, and chemistry. Lagrangian particle tracking of liquid fuel droplets was coupled with Eulerian simulation of the gas phase, where flow is governed by the Navier−Stokes equations. Turbulence was accounted for using a dynamic structure large eddy simulation turbulence model.[35] The walls were set at a constant temperature equal to the initial chamber temperature. Heat transfer between the walls and the air in the chamber comes primarily from the conduction term in the energy equation. The turbulent thermal conductivity that was used for heat transfer was defined as follows:

$$K_t = K + C_p \frac{\mu_t}{Pr_t}$$

where K_t is the turbulent thermal conductivity, K is the material thermal conductivity, C_p is the heat capacity, Pr_t is the turbulent Prandtl number (Pr_t = 0.9), and μ_t is the turbulent viscosity. The turbulent viscosity is a function of the sub-grid kinetic energy calculated by the turbulence model. The base mesh

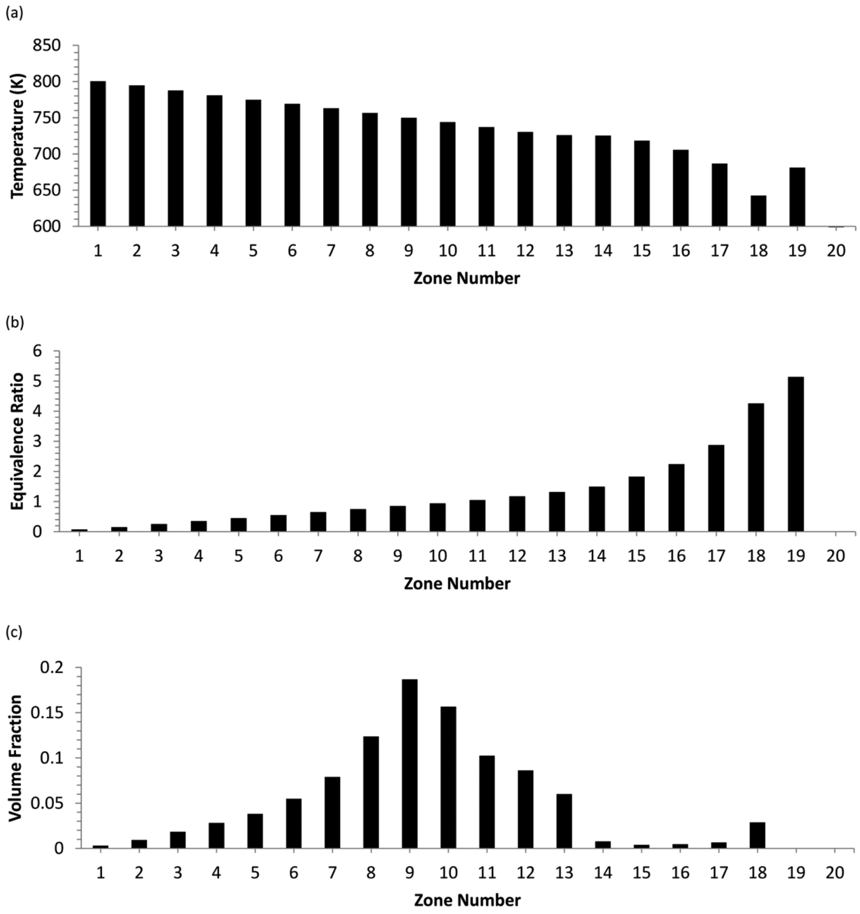

Figure 4. Example of (a) initial temperature, (b) equivalence ratio, and (c) volume fraction of different zones that were used as inputs for the multizone model. These data were taken from a CFD model run without chemistry at initial conditions of 823 K and 1.5 MPa at a time of 32 ms. Global φ = 0.9.

consisted of roughly 62 000 hexahedral cells. Automatic mesh refinement was used to refine the mesh in areas of large gradients in the temperature, equivalence ratio, or velocity up to a maximum of 200 000 cells. This model was run both with an 89 species reduced iso-octane kinetic mechanism and without chemistry. The mechanism reduction procedure is described in more detail below. All models used the same definition for the start of ignition as the experimental data (413 kPa above the initial pressure). CFD-without-chemistry simulations were performed to characterize the mixing inside of the IQT and to provide initial conditions for subsequent single-zone and multizone modeling. Input parameters for CFD modeling of the IQT, such as the spray droplet size, spray velocity, and spray cone angle, have been discussed in more detail previously.[33] Experimental validation of the CFD model at operational pressures is not performed because there is no optical access in the IQT.

3.2. Single-Zone Model. The CHEMKIN-PRO software package[36] was used to model the IQT using a single-zone homogeneous batch reactor model. This model does not allow for spatial variance. To improve the accuracy of the model from previous studies and to remove the uncertainty of initial conditions, the single-zone model was run with initial conditions predicted from the CFD-without-chemistry, which is discussed later.

3.3. Multizone Model. A multizone engine model using the CHEMKIN-PRO software package[36] with 20 zones was also used to model the IQT. The concepts for the multizone engine model were developed by Aceves et al.[37] The engine model was used because there is no multizone homogeneous batch reactor model in CHEMKIN-PRO. The displacement volume and engine speed were set to 1×10^{-10} cm^3 and 1 rpm, respectively. These parameter choices resulted in a system that was effectively a constant volume over the time frame investigated. Initial conditions for the temperature, equivalence ratio, and volume fraction of zones were provided by the CFD-without-chemistry simulations. These inputs allow us to take into account gradients in the temperature and equivalence ratio for which the single-zone model cannot account.

In the multizone engine model, there is no mass or heat transferred between the zones. However, all of the zones are at the same pressure. If there is heat generated in one zone, it compresses the other zones adiabatically until pressure is equalized. This can allow non-reacting zones that are too lean to ignite to absorb energy released by reacting zones, via compression work, which, in turn, can slow the overall ignition event (this effect may speed ignition in the NTC region). Alternatively, it can allow for rich zones that are small in size to heat other zones via compression to speed bulk ignition.

3.4. Initial Conditions for Single-Zone and Multizone Models. To provide initial conditions for the multizone model, the CFD domain needs to be split into smaller domains to define each zone. Temperatures, equivalence ratios, and volume fractions for each cell were extracted from the CFD-without-

DOI: 10.1021/acs.energyfuels.6b01406
Energy Fuels XXXX, XXX, XXX−XXX

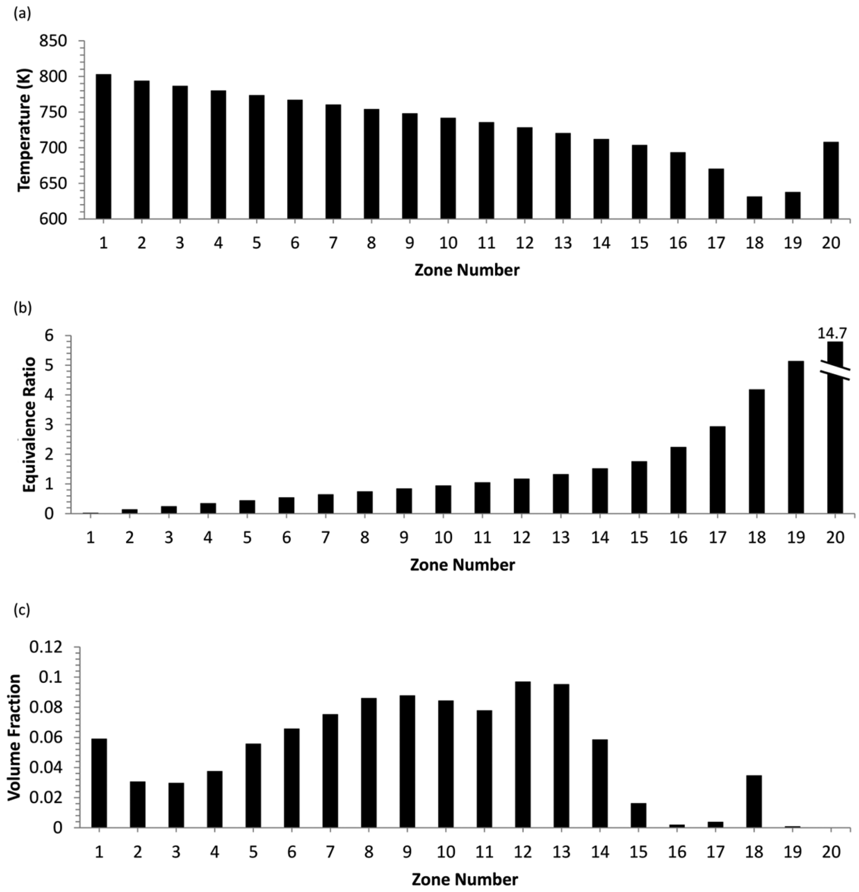

Figure 5. Example of (a) initial temperature, (b) equivalence ratio, and (c) volume fraction of different zones that were used as inputs for the multizone model. These data were taken from a CFD model run without chemistry at initial conditions of 823 K and 1.5 MPa at a time of 20 ms. Global φ = 0.9.

chemistry at a time that corresponded to the experimentally measured ignition delay time. The conditions in the chamber predicted by the CFD-without-chemistry varied significantly over time while the fuel and air in the chamber mixed. However, when conditions from different times (a few milliseconds apart from the experimental ignition delay time) were input into the multizone model, the ignition delay times predicted by the multizone model varied by only a few milliseconds. This suggests that changing the input conditions by a few miliseconds will not significantly affect the predicted ignition delay times. Also, whether the ignition delay time predicted by the multizone model increased or decreased, as the time used for inputs increased, was inconsistent between the conditions examined. This inconsistency could be due to predictions in the NTC region having the opposite trend compared to predictions outside the NTC region. The cells were divided into 20 different zones by equivalence ratio. Increasing the number of zones to 30 changed the predicted ignition delay time only by ~1%, showing that using 20 zones was adequate to model ignition behavior. Defining zones by temperature instead of equivalence ratio resulted in little difference in ignition delay time prediction. An equivalence ratio step size of 0.1 was chosen for equivalence ratios of $0 \leq \varphi \leq 1$. For $\varphi \geq 1$, the zone boundaries were equal to the inverse of the analogous equivalence ratio zone boundaries below 1 (i.e., 1/0.9 = 1.11, 1/0.8 = 1.25, 1/0.7 = 1.43, etc.). The reason for this change in step size was to allow rich zone boundaries to have the same relative change between them as the lean zone boundaries. Because the zones are defined only by the equivalence ratio, they do not represent a continuous volume inside the chamber. The initial conditions of each zone were calculated by the volume-weighted average of all of the cells with equivalence ratios between the two bounding equivalence ratio values. Some CFD predictions did not contain any cells at very rich or very lean conditions. This resulted in empty zones as inputs to the multizone model.

Inputs to the multizone model for one set of conditions (823 K, 1.5 MPa, t = 32 ms, and global φ = 0.9) are shown in Figure 4. Contour plots of the temperature and equivalence ratio including this set of conditions are discussed later (cf. Figure 9). Generally, the rich zones are in the back of the combustion chamber, and the leaner zones are in the main part of the combustion chamber. A small amount of heat transfer is seen by an increase in the temperature near the walls at long times. For these conditions, there were no cells in the CFD with an equivalence ratio of $\varphi \geq 10$. Therefore, zone 20 was input as empty in the multizone model, resulting in 19 zones with significant volume. The temperature and equivalence ratio are inversely related to each other as a result of evaporative cooling. The majority of the volume for this set of conditions is contained within zones 8−11. These zones are close to the global equivalence ratio (φ = 0.9), but they are significantly cooler (~75 K cooler) than the initial temperature.

While an approximate normal distribution for the volume fraction is apparent in Figure 4, a bimodal distribution exists at short times when fuel is concentrated in a small portion of the

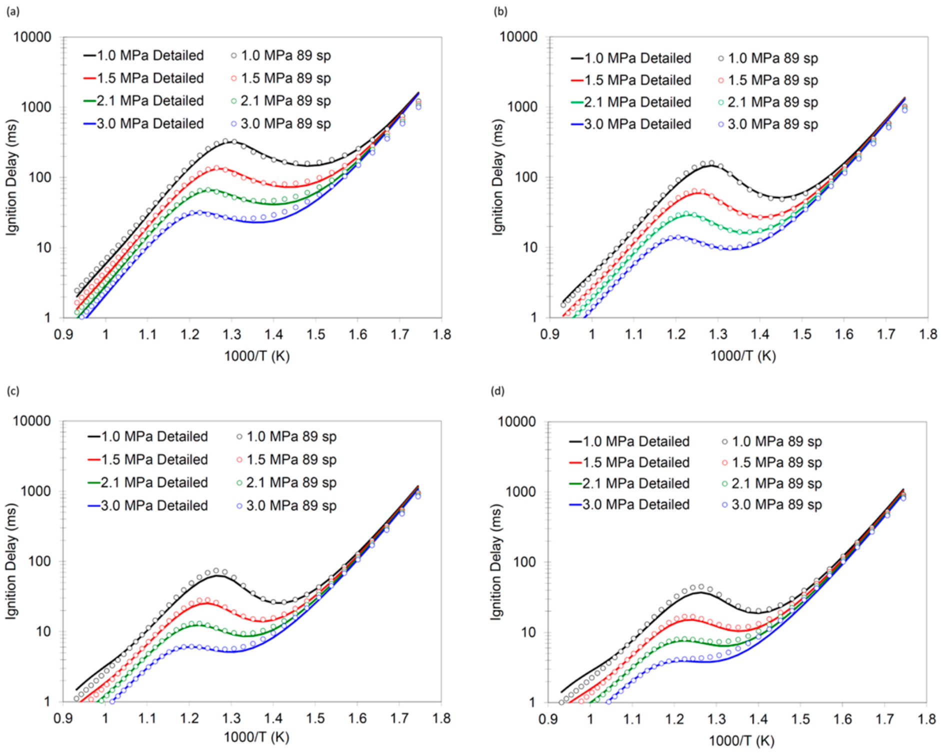

Figure 6. Comparison of 89 species reduced mechanism (dashed line) and detailed mechanism (solid line) for iso-octane ignition. Equivalence ratios are (a) 0.5, (b) 1, (c) 2, and (d) 3.

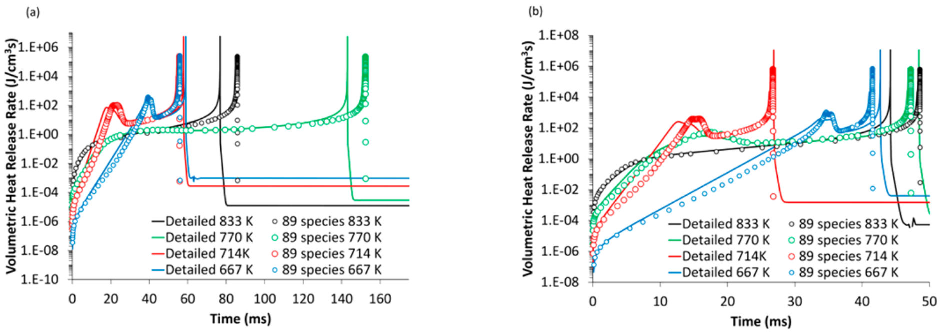

Figure 7. Volumetric heat release rate from model predictions for the 89 species reduced and detailed mechanisms at (a) 1.0 MPa and (b) 1.5 MPa. Φ = 1.

chamber; at longer times, the system will eventually have all of the volume in a single zone when the chamber is completely well-mixed. The multizone inputs taken at shorter times are shown in Figure 5. These conditions revealed that the volume fractionates into a bimodal distribution with additional peaks at very lean (zone 1) and very rich (zone 18) zones.

The single-zone CHEMKIN-PRO model also used the CFD-without-chemistry predictions to provide model inputs. A volume-weighted average of all of the cells in the CFD-without-chemistry simulation was used to generate a single temperature and equivalence ratio that was used as the initial condition for the single-zone model. For the conditions shown in Figure 4, the average temperature and equivalence ratio were 746.5 K and 0.98, respectively. These inputs using the CFD-without-chemistry simulations provide significantly more accurate model inputs than were used with the heptane isomer model.[19]

3.5. Reduction of the Iso-octane Mechanism.

The detailed 874 species iso-octane mechanism developed at Lawrence Livermore National Laboratory[20] was reduced to an 89 species mechanism. The CHEMKIN-PRO mechanism reduction code was used to perform the reduction. The 0D single-zone homogeneous batch reactor was used for the reduction. This code uses the directed relation graph[38−40] (DRG) and directed relation graph with error propagation[41] (DRGEP) methods to reduce the detailed mechanism. A sensitivity analysis, alone or coupled with DRG or DRGEP, was then used to further reduce the mechanism. Reduction was performed at 22 points across a temperature range of 673−1023 K, a pressure range of 1.5−3.0 MPa, and an equivalence ratio range of 0.5−2.0. These conditions were chosen to span the range of temperatures and equivalence ratios inside the IQT prior to ignition. The reduced mechanism was able to accurately reproduce the results of the detailed mechanism across the range of conditions tested, even outside of the 22 points used for reduction. The reduced mechanism agreed well with the detailed mechanism at all four equivalence ratios tested (0.5, 1, 2, and 3). A representative comparison of the detailed and reduced mechanisms is provided in Figure 6.

DOI: 10.1021/acs.energyfuels.6b01406

The volumetric heat release of the two mechanisms, shown in Figure 7, was also compared. The timing and magnitude of low-temperature heat release was predicted well for these conditions that are inside the NTC region. The entire profile for volumetric heat release matches well between the reduced and detailed mechanisms until very close to the ignition event. The differences in predicted ignition delay times for these conditions were less than 15%.

4. RESULTS AND DISCUSSION

4.1. Iso-octane Experimental Data. Iso-octane experiments were run in the IQT at two pressures, 1.0 and 1.5 MPa. While experiments on a wider range of pressures could be performed, these relatively low pressures provided ignition delay times that were long enough to reach quasi-homogeneous conditions inside the combustion chamber but not so long that wall effects may significantly affect the ignition delay times. While engines typically operate at higher pressure, the shorter ignition delay times at higher pressures mean that the spray physics is more important and it is much more difficult to assess the accuracy of the chemical mechanism. For a given pressure, the mass of fuel injected was kept the same across all temperatures, and as a result, the equivalence ratio changed between 0.7 and 1.05 across the range of temperatures characterized. The experimental temperature range (653−996 K) was chosen to capture the entire NTC region.

The NTC region is important in the low-temperature combustion of many hydrocarbon fuels. It is characterized by an increase (or flattening) of the ignition delay time as the temperature increases. This reduction in reactivity is due to alkyl radical + O_2 chemistry, which can lead to either chain branching, propagation, or inhibition reaction pathways. The competition between these pathways and shifting reaction equilibria are the major causes of NTC behavior.[42,43] As the temperature further increases, high-temperature ignition pathways begin to dominate, thereby decreasing the ignition delay time.

The experimental data for ignition delay times at 1.0 and 1.5 MPa can be seen in Figure 8. There is some uncertainty in the ignition delay time measurements, and the degree of uncertainty can be seen by the scatter of experimental ignition delay times with similar temperatures. NTC behavior can be clearly seen at both pressures indicated by the three regions with different slopes of ignition delay time versus inverse temperature. The data collected at 1.0 MPa have longer ignition delay times, and the NTC behavior is more pronounced. The observation of NTC behavior indicates that, under these conditions, chemical kinetics is more important than spray physics.

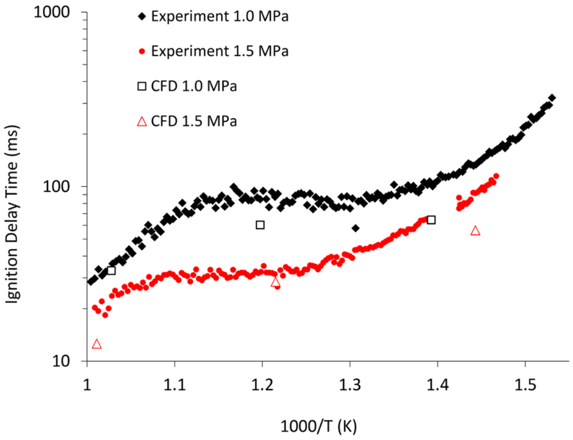

Figure 8. Experimental data (closed symbols) and coupled CFD−kinetics model predictions (open symbols). The 89 species reduced mechanism was used for model predictions, with 21% O_2 and $0.7 \leq \varphi \leq 1.05$.

4.2. Coupled CFD−Kinetics Modeling. The CFD model coupled with chemical kinetics using the 89 species reduced mechanism was compared to experimental ignition delay times. Because the coupled CFD−kinetics simulations took, on average, 5.3 days of computation time, only three temperatures were run at each pressure. A comparison between experimental and coupled CFD−kinetics model results can be seen in Figure 8. Although the coupled CFD−kinetics model predictions at 1.5 MPa capture the ignition delay time at one point in the NTC region, the predictions are too fast at higher and lower temperatures. At 1.0 MPa, the predictions at the lower temperatures are too fast and it appears that the extent of the NTC region might be too broad. It would be difficult to determine through coupled CFD−kinetics simulations whether these discrepancies are due to inadequacies in the chemical mechanism or inaccuracies within the CFD model, given the long simulation times. However, considering the CFD and chemical kinetics individually can provide more insight into the discrepancy between experimental and model results.

For most cases examined, the coupled CFD−kinetics model predicted multiple small flamelets forming near the walls. These flamelets started to propagate outward. Bulk autoignition was predicted before these flamelets could propagate across the entire chamber. The presence of flamelets near the wall suggests that heat transfer from the walls speeds ignition. Without optical access into the IQT, these predictions cannot be experimentally validated.

4.3. CFD-Without-Chemistry Modeling. CFD-without-chemistry simulations were run to characterize the mixing and evaporative cooling inside the IQT. The initial conditions run in the CFD model correspond to initial air temperature, pressure, and mass of fuel injected values for each experimental data point being modeled.

The predicted temperature and equivalence ratio contour plots for one set of conditions (823 K, 1.5 MPa, and global $\varphi = 0.9$) are shown in Figure 9. The experimentally measured and coupled CFD−kinetics simulation predicted ignition delay times for these conditions were 31.5 and 28.5 ms, respectively. At 4 ms, large gradients in the temperature and equivalence ratio are present and a significant amount of fuel had penetrated to the back of the chamber. However, by 20 ms, there are smaller gradients in the main part of the combustion chamber. At 32 ms, which is close the experimental ignition delay time, the main part of the chamber was fairly well-mixed. This part of the chamber is close to the global equivalence ratio for these conditions, but the temperature is roughly 75 K cooler than the initial temperature. The contour plots at 50 ms show slightly more uniform conditions within the chamber than at 32 ms. Most of the experimental ignition delay times discussed earlier are longer than 20 ms, and many are longer than 32 ms. Because the combustion chamber appears to be fairly well-mixed at these long times, one might expect that the predictions from the single-zone and/or multizone models would provide adequate descriptions of the system. Of course, the inclusion of multiple zones, each with its own temperature and equivalence ratio, should lead to an improved description.

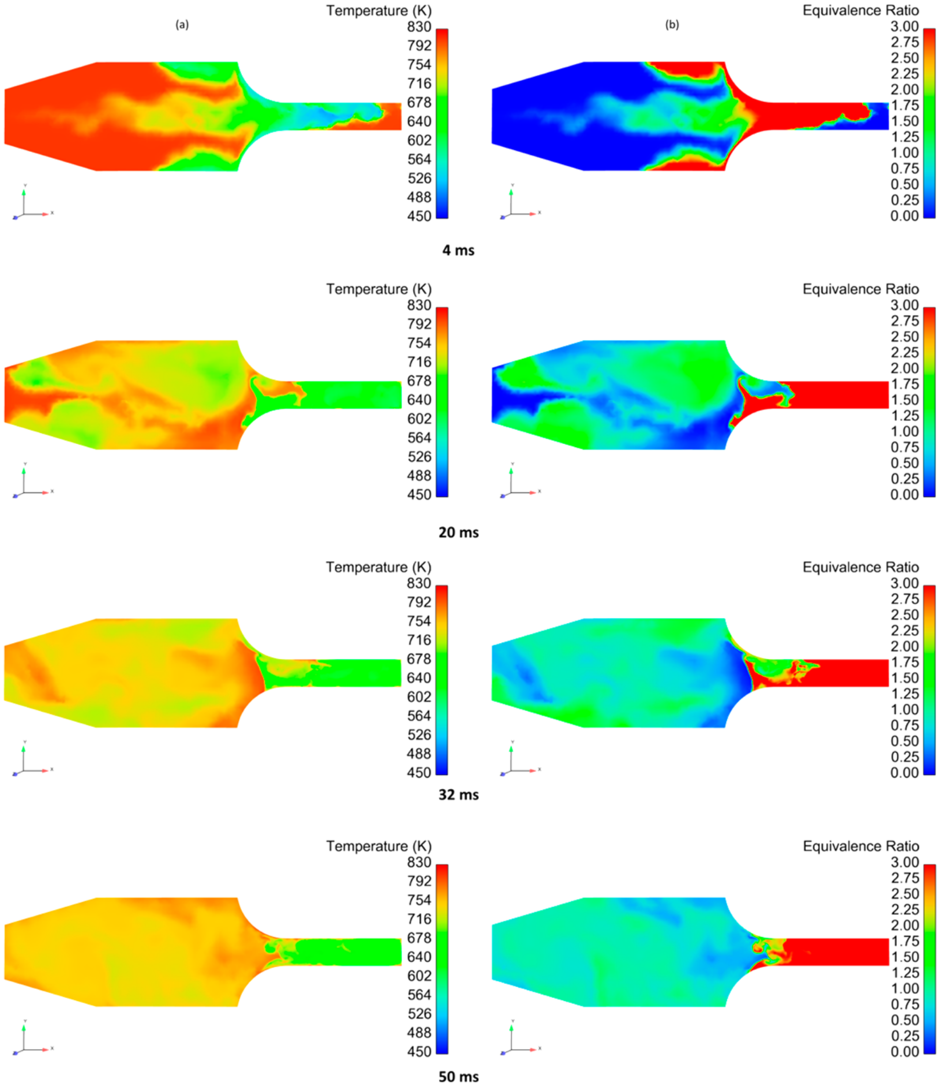

Figure 9. Contour plots of (a) temperature and (b) equivalence ratio for iso-octane at 1.5 MPa, 823 K, and global $\varphi = 0.9$. No chemistry was run. The experimental ignition delay time was 31.54 ms at these conditions.

The conditions inside the chamber at 32 ms were used as inputs (cf. Figure 4) into the single-zone and multizone CHEMKIN modeling discussed in section 4.4.

4.4. 0D Model Comparisons. The single-zone and multizone models were run at eight temperatures for each pressure. Comparisons of experimental and 0D-model-predicted ignition delay times are shown in Figure 10. The temperatures, in Figure 10, at which the single-zone and multizone models are plotted correspond to temperatures that were used as initial conditions in the CFD-without-chemistry simulations that provided the inputs for the single-zone and multizone models. These temperatures correspond to the experimentally measured temperatures that are recorded before fuel is injected. The single-zone model overemphasized the magnitude of the NTC effect at 1.0 MPa, but it captures the high-temperature observations. For the higher reactivity 1.5 MPa case, this model is less successful. It likely suffers from neglecting the presence of richer zones inside the chamber at the highest temperatures, where the experimental ignition delay time is only ~20 ms. It also predicts much more obvious NTC behavior than is observed and predicts much faster ignition at lower temperatures than is observed.

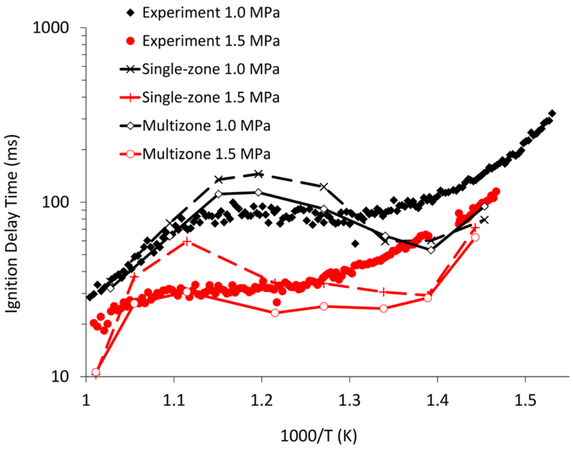

Figure 10. Experimental results (diamonds and circles) with single-zone (dashed lines) and multizone (solid lines) model predictions for iso-octane. The 89 species reduced mechanism was used for model predictions, with 21% O_2 and $0.7 \leq \varphi \leq 1.05$.

At both high and low temperatures, the predictions of the multizone model are similar to those of the single-zone version.

DOI: 10.1021/acs.energyfuels.6b01406
Energy Fuels XXXX, XXX, XXX−XXX

An improvement in the multizone model is that the overall shape is closer to the experimental shape than the single-zone model predictions. The multizone predictions at 1.5 MPa are much improved at higher temperatures, except the highest temperature modeled, but they become too fast at lower temperatures. For most cases, the multizone ignition delay time predictions are similar to or better than those of the single-zone model.

Comparisons of the coupled CFD−kinetics model and the multizone model are shown in Figure 11. At 1.5 MPa, the multizone model predictions for ignition delay time are very close to predictions made by the CFD model. Although the predictions are generally faster than observed, the good agreement between the CFD and multizone models suggests that the temperatures and equivalence ratios predicted using the CFD-without-chemistry model are appropriate for use as initial conditions in the multizone model. At 1.0 MPa, the CFD and multizone models are in good agreement at high and low temperatures. However, there is a significant difference in the model predictions between the CFD model and the multizone model in the NTC region. This difference requires further investigation. Inadequate prediction of low-temperature heat release could be a cause of the differences in prediction in the NTC region. The overall agreement indicates that the multizone model can account for the majority of the effects of incomplete mixing and evaporative cooling inside the IQT that are based on the CFD-without-chemistry results. The underprediction of ignition delay time for both the multizone and CFD models at longer ignition delay times may result from an overprediction of heat transfer into the combustion chamber. An investigation of heat transfer inside the IQT is currently ongoing. Also, these deviations may be due to deficiencies in the chemical mechanism because it had not been validated for rich equivalence ratio conditions that are present at some locations within the IQT.[32] Similarly, there could be problems with aspects of the spray/droplet/evaporation treatment in the CFD model.

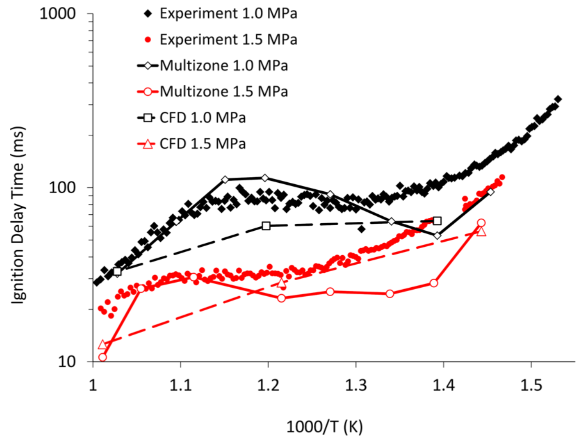

Figure 11. Experimental results (diamonds and circles) with CFD (open triangles and open squares) and multizone (solid lines) model predictions for iso-octane ignition. The 89 species reduced mechanism was used for model predictions, with 21% O_2 and $0.7 \leq \varphi \leq 1.05$.

Both the single-zone and multizone models appear significantly more accurate than the method that was used previously for heptane isomer modeling (cf. Figure 2) that did not use CFD-without-chemistry simulation results for model inputs.[19] However, to provide a fair comparison, a single-zone model was run with similar methodology as the model run for the heptane isomers. The single-zone model was run with experimentally measured temperatures, before fuel injection, and it was run at the global equivalence ratio and at double the global equivalence ratio to attempt to bound uncertainty with regard to mixing inside the chamber. A comparison of this older modeling methodology to the experimental results and multizone predictions is shown in Figure 12. Without any temperature correction in the old single-zone model to account for evaporative cooling, the ignition delay time prediction curve is shifted to lower temperatures relative to the experimental data. One could imagine shifting these curves to higher temperatures and finding reasonable accuracy at high and low temperatures. However, the magnitude of the NTC predicted by the old single-zone model is much larger than seen experimentally.

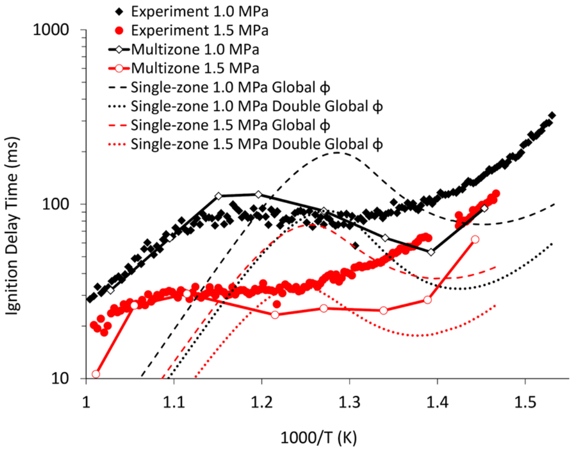

Figure 12. Experimental results (diamonds and circles) with multizone (solid lines) model predictions for iso-octane. Single-zone model, using an older methodology, at the global equivalence ratio (dashed line) and double the global equivalence ratio (dotted line). The 89 species reduced mechanism was used for model predictions, with 21% O_2 and global φ of $0.7 \leq \varphi \leq 1.05$.

The improved initial conditions for the multizone model allowed for more accurate ignition predictions, and the increased accuracy of the temperature estimate provides a way to adjust the model predictions, so that they can be compared at a similar temperature to the experimental data after fuel evaporation. Additionally, running the model at two different equivalence ratios was no longer needed to bound uncertainty in the equivalence ratio values. For the multizone model, inhomogeneity inside the IQT was taken into account, allowing for increased accuracy of ignition predictions.

4.5. Calculation Time Comparison. While the most accurate model is desirable, the calculation time is an important consideration. The calculation times and lengths of time that were modeled by the CFD models are listed in Table 1. Both sets of CFD calculations were run on the same computer using the same number of computational cores. The single-zone and multizone model calculation times (<1 min) are not shown because they are negligible compared to the CFD model calculation times. Thus, the amount of time to complete the multizone modeling would mainly come from the time to complete CFD-without-chemistry simulations to generate the model inputs. The CFD model generally took longer to calculate a solution at lower pressures partially because the

Table 1. Comparison Calculation Times for the CFD-Without-Chemistry and Coupled CFD−Kinetic Models and the Length of Time That Was Modeled

experimental conditions	CFD-without-chemistry calculation time (days)	coupled CFD−kinetics calculation time (days)	length of time modeled (ms)	ratio of calculation times: chemistry/no chemistry
1.0 MPa and 718 K	0.50	6.30	65	12.7
1.0 MPa and 835 K	0.52	7.42	61	14.3
1.0 MPa and 973 K	0.44	3.89	33	8.89
1.5 MPa and 693 K	0.53	4.11	57	7.80
1.5 MPa and 823 K	0.45	4.83	29	10.6
1.5 MPa and 989 K	0.45	5.37	13	12.0
average				11.1

model needed to be run out to longer times. The ratio of calculation times shows that, on average, a coupled CFD−kinetics simulation with chemistry takes ∼11 times longer than a CFD-without-chemistry simulation. Therefore, approximately 11 multizone model simulations (each requiring a CFD-without-chemistry run to provide inputs) could be performed for every coupled CFD−kinetics simulation. As a result, a comparison of experimental data and model results across a much broader range of conditions could be performed with the multizone model than with the coupled CFD−kinetics model, especially for larger chemical mechanisms. The CFD results with the 89 species mechanism indicate that additional improvements are required to fully characterize the IQT results for iso-octane. Using the multizone model approach should expedite the search for such improvements, because it will be feasible to test more conditions and more detailed mechanisms in a realistic time frame. This method may also be applied to low-volatility fuels, where it is more difficult to obtain data with traditional kinetics experiments but are readily obtained in the IQT. Thus, it would be possible to validate the larger kinetic mechanism associated with these larger fuel molecules.

5. CONCLUSION

Ignition delay times for iso-octane measured in an IQT showed clear NTC behavior. Three modeling methods were used to model these data. A reduced chemical mechanism for iso-octane containing 89 species was used in each approach. The results of the most complete model, a coupled CFD−kinetics model, captured the trends observed but predicted shorter ignition delays than experimentally observed at lower temperatures. The CFD-without-chemistry predictions showed a large quasi-homogeneous zone in the IQT at longer residence times. The presence of such a zone suggested that it may be possible to use a simple 0D kinetics calculation to predict the ignition delay times under these relatively long-time events. These types of calculations are much faster than those involving CFD, such that one can explore much more complex mechanisms over a wider range of conditions.

The temperatures and equivalence ratios in this quasi-homogeneous zone were then used as inputs for either single-zone or multizone model predictions. The multizone results were very similar in most cases to those using the coupled CFD−kinetics model, with the substantial advantage of requiring ∼11 times less central processing unit (CPU) time. These results suggest that the approach of using a detailed CFD-without-chemistry simulation to identify conditions where quasi-homogeneous zones exist would allow for the design of IQT experiments where the results could be interpreted in terms of simple 0D calculations. This could be valuable for testing detailed mechanisms of complex low-volatility fuels by comparison to IQT data on these fuels.

■ ASSOCIATED CONTENT

Ⓢ Supporting Information

The Supporting Information is available free of charge on the ACS Publications website at DOI: 10.1021/acs.energyfuels.6b01406.

89 species reduced mechanism (TXT)

■ AUTHOR INFORMATION

Corresponding Author

*E-mail: eosecky@mines.edu.

Notes

The authors declare no competing financial interest.

■ ACKNOWLEDGMENTS

This work was supported by the U.S. Department of Energy under Contract DE-AC36-08GO28308 with the National Renewable Energy Laboratory. Funding was provided by U.S. Department of Energy's Office of Energy Efficiency and Renewable Energy, Vehicle Technologies Office. The authors thank Convergent Science for providing a software license to CONVERGE at Colorado School of Mines for this analysis. The authors also thank Dr. Sibendu Som at Argonne National Laboratory for sharing initial input data that were used in the CONVERGE simulations.

■ REFERENCES

(1) Reitz, R. D.; Duraisamy, G. Review of high efficiency and clean reactivity controlled compression ignition (RCCI) combustion in internal combustion engines. *Prog. Energy Combust. Sci.* **2015**, *46*, 12−71.

(2) Wooldridge, M.; Walton, S.; He, X.; Zigler, B. T. Chemical kinetics of homogeneous charge compression ignition and other low-temperature combustion strategies. *Proceedings of the 2006 Technical Meeting of the Central States Section of the Combustion Institute*; Cleveland, OH, May 21−23, 2006.

(3) Westbrook, C. K.; Pitz, W. J.; Boercker, J. E.; Curran, H. J.; Griffiths, J. F.; Mohamed, C.; Ribaucour, M. Detailed chemical kinetic reaction mechanisms for autoignition of isomers of heptane under rapid compression. *Proc. Combust. Inst.* **2002**, *29*, 1311−1318.

(4) Mehl, M.; Pitz, W. J.; Westbrook, C. K.; Curran, H. J. Kinetic modeling of gasoline surrogate components and mixtures under engine conditions. *Proc. Combust. Inst.* **2011**, *33*, 193−200.

(5) Allen, C.; Mittal, G.; Sung, C. J.; Toulson, E.; Lee, T. An aerosol rapid compression machine for studying energetic-nanoparticle enhanced combustion of liquid fuels. *Proc. Combust. Inst.* **2011**, *33*, 3367−3374.

(6) Davidson, D. F.; Haylett, D. R.; Hanson, R. K. Development of an aerosol shock tube for kinetic studies of low-vapor-pressure fuels. *Combust. Flame* **2008**, *155*, 108−117.

(7) Oehlschlaeger, M. A.; Steinberg, J.; Westbrook, C. K.; Pitz, W. J. The autoignition of iso-cetane at high to moderate temperatures and elevated pressures: Shock tube experiments and kinetic modeling. *Combust. Flame* **2009**, *156* (11), 2165−2172.

(8) Won, S. H.; Dooley, S.; Veloo, P. S.; Wang, H.; Oehlschlaeger, M. A.; Dryer, F. L.; Ju, Y. The combustion properties of 2,6,10-trimethyldodecane and a chemical functional group analysis. *Combust. Flame* **2014**, *161*, 826−834.

(9) Ristori, A.; Dagaut, P.; Cathonnet, M. The oxidation of *n*-hexadecane: Experimental and detailed kinetic modeling. *Combust. Flame* **2001**, *125* (3), 1128−1137.

(10) ASTM International *ASTM D6890-16, Standard Test Method for Determination of Ignition Delay and Derived Cetane Number (DCN) of Diesel Fuel Oils by Combustion in a Constant Volume Chamber*; ASTM International: West Conshohocken, PA, 2016; www.astm.org.

(11) Bogin, G.; Dean, A. M.; Ratcliff, M. A.; Luecke, J.; Zigler, B. T. Expanding the experimental capabilities of the ignition quality tester for autoigniting fuels. *SAE Int. J. Fuels Lubr.* **2010**, *3*, 353−367.

(12) Haas, F. M.; Ramcharan, A.; Dryer, F. L. Relative reactivities of the isomeric butanols and ethanol in an ignition quality tester. *Energy Fuels* **2011**, *25* (9), 3909−3916.

(13) Heyne, J. S.; Boehman, A. L.; Kirby, S. Autoignition studies of *trans*- and *cis*-decalin in an ignition quality tester (IQT) and the development of a high thermal stability unifuel/single battlefield fuel. *Energy Fuels* **2009**, *23*, 5879−5885.

(14) Guillen, D. P. The autoignition of cyclopentane in an ignition quality tester. *JOM* **2012**, *64* (8), 985−989.

(15) Zheng, Z.; Badawy, T.; Henein, N.; Sattler, E. *Investigation of Physical and Chemical Delay Period of Different Fuels in the Ignition Quality Tester (IQT)*; Defense Technical Information Center: Fort Belvoir, VA, 2012; ADA574671, http://handle.dtic.mil/100.2/ADA574671.

(16) Perez, P. L.; Boehman, A. L. Experimental investigation of the autoignition behavior of surrogate gasoline fuels in a constant-volume combustion bomb apparatus and its relevance to HCCI combustion. *Energy Fuels* **2012**, *26* (10), 6106−6117.

(17) Bogin, G. E., Jr.; Osecky, E.; Chen, J. Y.; Ratcliff, M. A.; Luecke, J.; Zigler, B. T.; Dean, A. M. Experiments and computational fluid dynamics modeling analysis of large *n*-alkane ignition kinetics in the ignition quality tester. *Energy Fuels* **2014**, *28* (7), 4781−4794.

(18) Ra, Y.; Reitz, R. D. A reduced chemical kinetic model for IC engine combustion simulations with primary reference fuels. *Combust. Flame* **2008**, *155*, 713−738.

(19) Bogin, G.; Osecky, E.; Ratcliff, M.; Luecke, J.; He, X.; Zigler, B. T.; Dean, A. M. Ignition quality tester (IQT) investigation of the negative temperature coefficient region of alkane autoignition. *Energy Fuels* **2013**, *27* (3), 1632−1642.

(20) Mehl, M.; Curran, H. J.; Pitz, W. J.; Westbrook, C. K. Chemical kinetic modeling of component mixtures relevant to gasoline. *Proceedings of the European Combustion Meeting*; Vienna, Austria, April 14−17, 2009.

(21) He, X.; Donovan, M. T.; Zigler, B. T.; Palmer, T. R.; Walton, S. M.; Wooldridge, M. S.; Atreya, A. An experimental and modeling study of iso-octane ignition delay times under homogeneous charge compression ignition conditions. *Combust. Flame* **2005**, *142*, 266−275.

(22) Walton, S. M.; He, X.; Zigler, B. T.; Wooldridge, M. S.; Atreya, A. An experimental investigation of iso-octane ignition phenomena. *Combust. Flame* **2007**, *150*, 246−262.

(23) Minetti, R.; Carlier, M.; Ribaucour, M.; Therssen, E.; Sochet, L. E. Comparison of oxidation and autoignition of the two primary reference fuels by rapid compression. *Symp. Combust., [Proc.]* **1996**, *26*, 747−753.

(24) Davidson, D. F.; Gauthier, B. M.; Hanson, R. K. Shock tube ignition measurements of iso-octane/air and toluene/air at high pressures. *Proc. Combust. Inst.* **2005**, *30*, 1175−1182.

(25) Davidson, D. F.; Oehlschlaeger, M. A.; Herbon, J. T.; Hanson, R. K. Shock tubes measurements of iso-octane ignition times and OH concentration time histories. *Proc. Combust. Inst.* **2002**, *29*, 1295−1301.

(26) Mittal, G.; Sung, C. A rapid compression machine for chemical kinetics studies at elevated pressures and temperatures. *Combust. Sci. Technol.* **2007**, *179*, 497−530.

(27) Dagaut, P.; Reuillon, M.; Cathonnet, M. High pressure oxidation of liquid fuels from low to high temperature. 1. *n*-Heptane and iso-octane. *Combust. Sci. Technol.* **1993**, *95*, 233−260.

(28) Griffiths, J. F.; Halford-Maw, P. A.; Mohamed, C. Spontaneous ignition delays as a diagnostic of the propensity of alkanes to cause engine knock. *Combust. Flame* **1997**, *111* (4), 327−337.

(29) Mittal, G.; Sung, C. A rapid compression machine for chemical kinetics studies at elevated pressures and temperatures. *Combust. Sci. Technol.* **2007**, *179*, 497−530.

(30) Petersen, E. L.; Lamnaouer, M.; de Vries, J.; Curran, H.; Simmie, J.; Fikri, M.; Schulz, C.; Bourque, G. Discrepancies between shock tube and rapid compression machine ignition at low temperatures and high pressures. In *Shock Waves*; Hannemann, K., Seiler, F., Ed.; Springer: Berlin, Germany, 2009; pp 739−744, DOI: 10.1007/978-3-540-85168-4_119.

(31) Fieweger, K.; Blumenthal, R.; Adomeit, G. Self-ignition of S.I. engine model fuels: A shock tube investigation at high pressure. *Combust. Flame* **1997**, *109* (4), 599−619.

(32) Curran, H. J.; Gaffuri, P.; Pitz, W. J.; Westbrook, C. K. A comprehensive modeling study of iso-octane oxidation. *Combust. Flame* **2002**, *129*, 253−280.

(33) Bogin, G. E., Jr.; DeFilippo, A.; Chen, J. Y.; Chin, G.; Luecke, J.; Ratcliff, M. A.; Zigler, B. T.; Dean, A. M. Numerical and experimental investigation of *n*-heptane autoignition in the ignition quality tester (IQT). *Energy Fuels* **2011**, *25* (12), 5562−5572.

(34) Richards, K. J.; Senecal, P. K.; Pomraning, E. *CONVERGE (Version 2.3)*; Convergent Science: Madison, WI, 2015.

(35) Pomraning, E. Development of large eddy simulation turbulence models. Ph.D. Thesis, University of Wisconsin—Madison, Madison, WI, 2000.

(36) Reaction Design. *CHEMKIN-PRO 15131*; Reaction Design: San Diego, CA, 2013.

(37) Aceves, S.; Flowers, D.; Martinez-Frias, J.; Smith, J. R.; Westbrook, C. K.; Pitz, W. J.; Dibble, R.; Wright, J. F.; Akinyemi, W. C.; Hessel, R. P. A sequential fluid mechanic chemical-kinetic model of propane HCCI combustion. *SAE Tech. Pap. Ser.* **2001**, DOI: 10.4271/2001-01-1027.

(38) Lu, T.; Law, C. K. A directed relation graph method for mechanism reduction. *Proc. Combust. Inst.* **2005**, *30* (1), 1333−1341.

(39) Lu, T.; Law, C. K. Linear time reduction of large kinetic mechanisms with directed relation graph: *n*-Heptane and iso-octane. *Combust. Flame* **2006**, *144*, 24−36.

(40) Lu, T.; Law, C. K. On the applicability of directed relation graphs to the reduction of reaction mechanisms. *Combust. Flame* **2006**, *146*, 472−483.

(41) Pepiot-Desjardins, P.; Pitsch, H. An efficient error-propagation-based reduction method for large chemical kinetic mechanisms. *Combust. Flame* **2008**, *154* (1−2), 67−81.

(42) Simmie, J. M. Detailed chemical kinetics models for the combustion of hydrocarbon fuels. *Prog. Energy Combust. Sci.* **2003**, *29*, 599−634.

(43) Curran, H. J.; Gaffuri, P.; Pitz, W. J.; Westbrook, C. K. A comprehensive modeling study of *n*-heptane oxidation. *Combust. Flame* **1998**, *114*, 149−177.

DOI: 10.1021/acs.energyfuels.6b01406
Energy Fuels XXXX, XXX, XXX−XXX